

© 2021. M.A. Giżejowski, A.M. Barszcz, Z. Stachura.

This is an open-access article distributed under the terms of the Creative Commons Attribution-NonCommercial-NoDerivatives License (CC BY-NC-ND 4.0, <https://creativecommons.org/licenses/by-nc-nd/4.0/>), which permits use, distribution, and reproduction in any medium, provided that the Article is properly cited, the use is non-commercial, and no modifications or adaptations are made.



ELASTIC FLEXURAL-TORSIONAL BUCKLING OF STEEL I-SECTION MEMBERS UNRESTRAINED BETWEEN END SUPPORTS

M. A. GIŻEJOWSKI¹, A. M. BARSZCZ², Z. STACHURA³

Elastic instability of steel I-section members has been investigated with regard to axial compression, major axis bending as well as compression and major axis bending, based on the Vlasov theory of thin-walled members. Investigations presented in this paper deal with the energy method applied to the flexural-torsional buckling (FTB) problems of any complex loading case that for convenience of predictions is treated as a superposition of symmetric and antisymmetric components. Firstly, the review of energy equation formulations is presented for the elastic lateral-torsional buckling (LTB) of beams, then the most accurate beam energy equation, so-called the classical energy equation formulated for bisymmetric I-section beams is extended to cover also the beam-column out-of-plane stability problems, referred hereafter to FTB problems. Secondly, for the simple end boundary conditions, the shape functions of twist rotation and minor axis displacement are chosen such that they cover both symmetric and antisymmetric lateral-torsional buckling modes in relation to two lowest eigenvalues of the beam LTB in major axis bending. Finally, the explicit form of the general solution is presented being dependent upon the dimensionless bending moment equations for symmetric and antisymmetric components, and the load factor ψ_k where the lower k index identifies the load case.

Keywords: steel member, bisymmetric I-section, elastic behaviour, lateral-torsional buckling, classical energy equation, flexural-torsional buckling

¹ Prof., DSc., PhD., Eng., Warsaw University of Technology, Faculty of Civil Engineering, Al. Armii Ludowej 16, 00-637 Warsaw, Poland, e-mail: m.gizejowski@il.pw.edu.pl

² PhD., Eng., Warsaw University of Technology, Faculty of Civil Engineering, Al. Armii Ludowej 16, 00-637 Warsaw, Poland, e-mail: a.barszcz@il.pw.edu.pl

³ MSc., Eng., Warsaw University of Technology, Faculty of Civil Engineering, Al. Armii Ludowej 16, 00-637 Warsaw, Poland, e-mail: z.stachura@il.pw.edu.pl

1. INTRODUCTION

The inelastic buckling strength of real steel members (members with realistic measures of material and geometric imperfections) is nowadays presented in the form of equations in which the elastic buckling solution of the perfect elastic member is an important model parameter. In order to relate the member inelastic resistance to the member upper bound limit, the member elastic buckling stress resultants are normalized with use of the respective section plastic resistances that correspond to the formation of a plastic hinge under a single stress resultant action effect or under multiple stress resultant action effects. The reference is made hereafter to Eurocode 3, Part 1-1 [5] for: (1) the column buckling resistance (clause 6.3.1), (2) the LTB resistance of beams under major axis bending (cf. the so-called General case of LTB assessment according to clause 6.3.2.2) and (3) the FTB resistance of beam-columns under combined compression and major axis bending (cf. the so-called General method of clause 6.3.4). The latter case of the member flexural-torsional buckling resistance is that encompassing the former two cases of buckling resistances being the extreme situations of the member buckling under compression and major axis bending, respectively. The elastic FTB problem is that of a general nature for the practical assessment of inelastic buckling resistance of real beam-columns, therefore it is the subject of investigations in this paper.

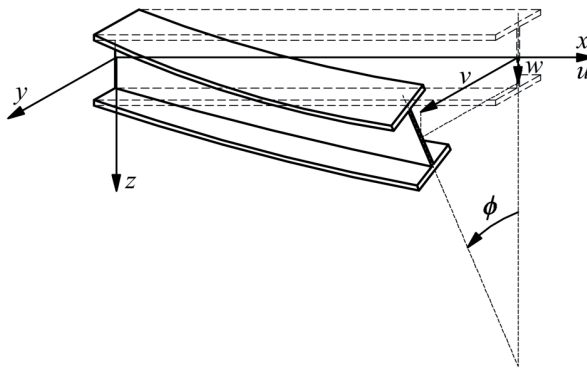


Fig. 1. Coordinate system used in beam theory

The use of energy methods in buckling problems is widely studied by Trahair [13]. Different approaches for the evaluation of proper equations of the elastic lateral-torsional buckling of beams was studied by Pi at al. [10] and Torkamani and Roberts [14]. The coordinate system referred to and used hereafter is that given in Fig. 1. Two energy equations were confronted in [10] in relation to

different description of displacement field approximations. The so-called alternative energy equation for LTB of beams subjected to in-plane distributed load q_{zi} acting in the range from $x_{qi,1}$ to $x_{qi,2}$ of the member length, and at the distance z_{qi} for the section shear centre, as well as to concentrated forces Q_{zj} acting at the distance x_{Qj} from the member axis origin, and at the distance z_{Qj} from the section shear centre, was written down in the following form:

$$(1.1) \quad \frac{1}{2} \int_0^L [EI_z \delta[(v'')^2] + EI_w \delta[(\phi'')^2] + GI_T \delta[(\phi')^2] - 2M_y \delta(v' \phi')] dx + \frac{1}{2} \sum_i \int_{x_{qi,1}}^{x_{qi,2}} q_{zi} z_{qi} \delta(\phi^2) dx + \frac{1}{2} \sum_j Q_{zj} z_{Qj} \delta \{ [\phi(x_{Qj})]^2 \} = 0$$

where:

E , G – Young modulus and Kirchhoff modulus of steel, I_z , I_w , I_T – minor axis moment of inertia, warping constant and Saint Venant torsion constant, $M_y = \int \sigma z dA$ – x -coordinate dependent prebuckling major axis bending stress resultant, A – cross-sectional area, L – element length, σ – prebuckling stress, v – minor axis flexural displacement (along y -axis), ϕ – mean twist rotation, δ – symbol of variation of the variable in the following parenthesis.

The results from Eq. (1.1) were compared in [10] with those obtained from the utilization of the so-called classical energy equation used for the linear eigenproblem analysis (LEA):

$$(1.2) \quad \frac{1}{2} \int_0^L \{ EI_z \delta[(v'')^2] + EI_w \delta[(\phi'')^2] + GI_T \delta[(\phi')^2] + 2M_y \delta(v'' \phi) \} dx + \frac{1}{2} \sum_i \int_{x_{qi,1}}^{x_{qi,2}} q_{zi} z_{qi} \delta(\phi^2) dx + \frac{1}{2} \sum_j Q_{zj} z_{Qj} \delta \{ [\phi(x_{Qj})]^2 \} = 0$$

Eq. (1.1) leads to an overestimation of the buckling load, sometimes unacceptable from engineering applications point of view, if compared with that from Eq. (1.2). In FTB analysis of beam-columns by the energy method, Eq. (1.2) is therefore used with the extension accounting for the influence of prebuckling axial stress resultant. Eq. (1.2) is dependent linearly upon the prebuckling stress resultant M_y , therefore it leads to an approximation of the buckling state within the linear buckling analysis (LBA) and formulated in the form of linear eigenproblem analysis (LEA).

Cuk and Trahair [4], and Gizejowski et al. [6] presented elastic buckling solutions for beam-columns under unequal end moments. Bijak solved the elastic buckling problems of beams [1] and beam-columns [2] using a modified Bubnov-Galerkin method. Many practical solutions for contemporary design applications have been collected by Trahair et al. [17]. The effect of

prebuckling flexural displacements on the elastic FTB behaviour is discussed by Mohri et al. [8,9] using conventional Bubnov-Galerkin method. With use of the energy method, the stability region of beam-columns with bisymmetric cross-sections and under combined loading represented by the axial force, uniformly distributed transverse loads and end bending moments was studied by Van Binh et al. [15]. Different aspects related to the formulation of buckling eigenproblems have been recently discussed by Gizejowski and Uziak [7].

The classical energy equation is widely utilized in the finite element formulation that is not limited to the elastic range only but also to inelastic out-of-plane buckling problems of beams and beam-columns, e.g. refer to Bradford et al. [3]. More recently, out-of-plane problems of elastic and inelastic buckling were formulated within the framework of nonlinear buckling analysis (NBA), e.g. Pi and Trahair [12, 13], Pi and Bradford [11]. These aspects are not considered in the present study. Elastic FTB problems are dealt with in this study using the classical energy method. Single loading and combined loading cases for members with simple boundary conditions are dealt with. The general solution is obtained by splitting any arbitrary asymmetric loading case into two components, symmetric and antisymmetric, in order to conveniently obtain the buckling limit curve relationship under the maximum moment and the compressive force. The symmetric and antisymmetric bending moment equations are set to be dependent upon the load factor ψ_k where the lower k index identifies the load case: $k = M$ for unequal end moments, $k = q$ for span uniformly distributed loads and $k = Q$ for span concentrated loads. The developed general solution encompasses coefficients that are listed for different loading cases and compared with results available in literature, wherever available.

2. PROBLEM FORMULATION

2.1. CLASSICAL ENERGY EQUATION AND ITS GENERAL SOLUTION

The classical energy conservation equation that provided a basis for the modern finite element method of FTB analysis is a simple extension of Eq. (1.2). It has been presented by Trahair [16]:

$$\begin{aligned}
 (2.1) \quad & \frac{1}{2} \int_0^L \{ EI_z \delta[(v'')^2] + EI_w \delta[(\phi'')^2] + GI_T \delta[(\phi')^2] + 2M_y \delta(v'' \phi) \} dx \\
 & - \frac{1}{2} N \int_0^L \{ \delta[(v')^2] + i_0^2 \delta[(\phi')^2] \} dx \\
 & + \frac{1}{2} \sum_i \int_{x_{qi,1}}^{x_{qi,2}} q_{zi} z_{qi} \delta(\phi^2) dx + \frac{1}{2} \sum_j Q_{zj} z_{Qj} \delta \{ [\phi(x_{Qj})]^2 \} = 0
 \end{aligned}$$

where:

$N = \int \sigma dA$ – prebuckling axial stress resultant, i_0 – polar radius of gyration accounting for the Wagner effect.

In the following, the simple member kinematic boundary conditions are dealt with, for which the twist rotation and transverse translations along section principal axes are fully restrained at both ends, while the flexural deflections about both section principal axes and warping are there allowed. The buckling twist rotation and minor axis flexural displacement are globally represented by trigonometric sinus functions, satisfying natural boundary conditions and approximating the LTB buckled shapes under symmetric M_{ys} and antisymmetric M_{ya} components of the x -coordinate dependent bending moment equation M_y . It has been proven in [16] that for solving the LEA elastic buckling problems of I-section beams under unequal end moments, the mean twist rotation ϕ is the exact half-wave sine function while the profile of minor axis displacements v changes shape from that of the exact half-wave for the equal and opposite end moments (uniform bending), to that of a wave one for the equal end moments of the same direction (antisymmetric bending). Hence, such trigonometric sinus shape functions widely used in literature are also adopted hereafter:

$$(2.2) \quad v = a_1 \sin(\pi\xi) + a_2 \sin(2\pi\xi)$$

$$(2.3) \quad \phi = a_3 \sin(\pi\xi)$$

where:

ξ – dimensionless coordinate equal to x/L , a_1 , a_2 and a_3 – unknown buckled shape constants.

Substituting Eqs. (2.2) and (2.3) to Eq. (2.1), the matrix LEA representation of the stability energy based equation is obtained:

$$(2.4) \quad \delta \mathbf{a}^T \mathbf{K}_{op} \mathbf{a} = \delta \mathbf{a}^T (\mathbf{K} + \alpha_{cr} \mathbf{K}_\sigma) \mathbf{a} = 0$$

where:

\mathbf{a} – vector of the unknown buckled shape constants (\mathbf{a}^T is that vector transposed):

$$\mathbf{a} = \begin{Bmatrix} a_1 \\ a_2 \\ a_3 \end{Bmatrix},$$

\mathbf{K}_{op} – out-of-plane stability stiffness matrix being the sum of the constitutive component \mathbf{K} and the initial stress component \mathbf{K}_σ , the latter dependent upon the reference values of prebuckling stress resultants N_0 and M_{y0} as well as in-plane loads $q_{zi,0}$ and $Q_{zi,0}$, α_{cr} – critical load factor.

The stiffness matrix components are of the following form:

- component \mathbf{K} :

$$\mathbf{K} = \begin{bmatrix} \frac{\pi^4 EI_z}{L^3} \int_0^1 \sin^2 \pi \xi d\xi & 0 & 0 \\ \text{symm.} & \frac{16\pi^4 EI_z}{L^3} \int_0^1 \sin^2 2\pi \xi d\xi & 0 \\ \text{symm.} & \text{symm.} & \frac{\pi^4 EI_w}{L^3} \int_0^1 \sin^2 \pi \xi d\xi + \frac{\pi^2 G I_T}{L} \int_0^1 \cos^2 \pi \xi d\xi \end{bmatrix}$$

- component \mathbf{K}_σ :

$$\mathbf{K}_\sigma = \begin{bmatrix} -\frac{\pi^2 N_0}{L} \int_0^1 \cos^2 \pi \xi d\xi & 0 & -\frac{\pi^2}{L} \int_0^1 M_{y0}(\xi) \sin^2 \pi \xi d\xi \\ \text{symm.} & -\frac{4\pi^2 N_0}{L} \int_0^1 \cos^2 2\pi \xi d\xi & -\frac{4\pi^2}{L} \int_0^1 M_{y0}(\xi) \sin \pi \xi \sin 2\pi \xi d\xi \\ \text{symm.} & \text{symm.} & -\frac{\pi^2 N_0 t_0^2}{L} \int_0^1 \cos^2 \pi \xi d\xi \end{bmatrix}$$

For nonzero values of the buckled shape constants, the critical load factor is calculated from the condition of equating the determinant of the out-of-plane stability stiffness matrix \mathbf{K}_{op} to zero. For hand calculations, it is more convenient to operate on the out-of-plane stability stiffness, instead on the stiffness matrix components, in order to directly derive the relationship between $M_{y,\max}$ and N . It describes directly the stability limit curve, instead evaluating the critical load factor α_{cr} and then finding the pair of critical values of $M_{y,\max} = \alpha_{cr} M_{y0,\max}$ and $N = \alpha_{cr} N_0$. The stability limit curve gives the critical values of a single stress resultant for two extreme points of that curve, namely $N = N_z$ for $M_{y,\max} = 0$ and $M_{y,\max} = M_{cr}$ for $N = 0$, where N_z is the minor axis flexural critical force and M_{cr} is the critical moment of lateral-torsional buckling. Expanding the determinant of the out-of-plane stiffness matrix \mathbf{K}_{op} and notifying that for adopted shape functions $K_{op}(1,2) = K_{op}(2,1) = 0$, one can obtain:

$$(2.5) \quad \det \mathbf{K}_{op} = 0 \rightarrow K_{op}(3,3) - \left\{ \frac{[K_{op}(1,3)]^2}{K_{op}(1,1)} + \frac{[K_{op}(2,3)]^2}{K_{op}(2,2)} \right\} = 0$$

where for load cases of end moments and/or span loads applied at the shear centre:

– diagonal terms are structured from the constitutive stiffness components:

$$\begin{aligned}
 K_{op}(1,1) &= \frac{\pi^4 E I_z}{L^3} \int_0^1 \sin^2 \pi \xi d\xi - \frac{\pi^2 N}{L} \int_0^1 \cos^2 \pi \xi d\xi = \frac{\pi^2}{2L} \left(\frac{\pi^2 E I_z}{L^2} - N \right) = N_z \left(1 - \frac{N}{N_z} \right) \frac{\pi^2}{2L} \\
 K_{op}(2,2) &= \frac{16\pi^4 E I_z}{L^3} \int_0^1 \sin^2 2\pi \xi d\xi - \frac{4\pi^2 N}{L} \int_0^1 \cos^2 2\pi \xi d\xi = \frac{2\pi^2}{L} \left(\frac{4\pi^2 E I_z}{L^2} - N \right) = N_{za} \left(1 - \frac{N}{N_{za}} \right) \frac{2\pi^2}{L} \\
 K_{op}(3,3) &= \frac{\pi^4 E I_w}{L^3} \int_0^1 \sin^2 \pi \xi d\xi + \frac{\pi^2 (G I_T - i_0^2 N)}{L} \int_0^1 \cos^2 \pi \xi d\xi = \frac{\pi^2}{2L} \left(\frac{\pi^2 E I_w}{L^2} + G I_T - i_0^2 N \right) = \\
 &= i_0^2 N_T \left(1 - \frac{N}{N_T} \right) \frac{\pi^2}{2L}
 \end{aligned}$$

– nonzero off-diagonal terms are those related to the initial stress resultant stiffness components:

$$\begin{aligned}
 K_{op}(1,3) = K_{op}(3,1) &= -\frac{\pi^2}{L} \int_0^1 [M_{ys}(\xi)] \sin^2 \pi \xi d\xi - \frac{\pi^2}{L} \int_0^1 [M_{ya}(\xi)] \sin^2 \pi \xi d\xi = -\frac{\pi^2}{L} M_{ys, \max} I_s \\
 K_{op}(2,3) = K_{op}(3,2) &= -\frac{4\pi^2}{L} \int_0^1 [M_{ys}(\xi)] \sin \pi \xi \sin 2\pi \xi d\xi - \frac{4\pi^2}{L} \int_0^1 [M_{ya}(\xi)] \sin \pi \xi \sin 2\pi \xi d\xi = \\
 &= -\frac{4\pi^2}{L} M_{ya, \max} I_a
 \end{aligned}$$

and $M_{ys, \max}$, $M_{ya, \max}$ – maximum absolute values of symmetric and antisymmetric moment components, scaling the elementary action field moment effects, $I_s = \int_0^1 \left[\frac{M_{ys}(\xi)}{M_{ys, \max}} \right] \sin^2(\pi \xi) d\xi$ – symmetric moment integral, $I_a = \int_0^1 \left[\frac{M_{ya}(\xi)}{M_{ya, \max}} \right] \sin(\pi \xi) \sin(2\pi \xi) d\xi$ – antisymmetric moment integral, N_{za} – second lowest bifurcation load equal to $4N_z$.

Rearranging Eq. (2.5) for load cases of end moments and/or span loads applied at the section shear centre, the following general relationship is obtained:

$$(2.6) \quad i_0^2 N_T N_z \left(1 - \frac{N}{N_T} \right) = \frac{(2M_{ys, \max} I_s)^2}{1 - \frac{N}{N_z}} + \frac{(2M_{ya, \max} I_a)^2}{1 - 0.25 \frac{N}{N_z}}$$

It has to be notified that for n symmetric and m antisymmetric moment components, the integrals constituting the off-diagonal terms of the out-of-plane stiffness matrix \mathbf{K}_{op} are the summation of n integrals for symmetric moments $M_{ys,i}(\xi)$ and m integrals for antisymmetric moments $M_{ya,j}(\xi)$. Introducing the maximum first order moment $M_{y, \max}$ and regarding that the critical moment $M_{cr,0}$ for the uniform bending is given by:

$$(2.7) \quad M_{cr,0} = i_0 \sqrt{N_T N_z}$$

Eq. (2.6) takes the form:

$$(2.8a) \quad \left(\frac{M_{y,\max}}{M_{cr,0}} \right)^2 \left[\left(\sum_{i=1}^n \frac{M_{ys,i,\max}}{M_{y,\max}} 2I_{si} \right)^2 + \frac{1 - \frac{N}{N_z}}{1 - 0.25 \frac{N}{N_z}} \left(\sum_{j=1}^m \frac{M_{ya,j,\max}}{M_{y,\max}} 2I_{aj} \right)^2 \right] = \left(1 - \frac{N}{N_z} \right) \left(1 - \frac{N}{N_T} \right)$$

or in the shortened form, similar to that obtained for the lateral-torsional buckling of beams:

$$(2.8b) \quad \left(\frac{M_{y,\max}}{C_{bc} M_{cr,0}} \right)^2 \frac{1}{F(N)} = 1$$

where:

$M_{y,\max}$ – maximum absolute value of the combined action moment effect scaling the field moment effects,

$F(N) = \left(1 - \frac{N}{N_z} \right) \left(1 - \frac{N}{N_T} \right)$ – coefficient representing the effect of out-of-plane buckling under compressive force on the LTB buckling moment, C_{bc} – factor converting arbitrary moment gradient cases into an equivalent uniform moment case.

The equivalent uniform moment factor C_{bc} depends upon the moment distributions $M_{ys}(\xi)$ and $M_{ya}(\xi)$. Moreover, it is varying with the minor axis critical force utilization ratio N/N_z as given below:

$$(2.9a) \quad \frac{1}{C_{bc}} = \left[\left(\frac{M_{ys,\max}}{M_{y,\max}} \sum_{i=1}^n \frac{M_{ys,i,\max}}{M_{ys,\max}} 2I_{si} \right)^2 + \frac{1 - \frac{N}{N_z}}{1 - 0.25 \frac{N}{N_z}} \left(\frac{M_{ya,\max}}{M_{y,\max}} \sum_{j=1}^m \frac{M_{ya,j,\max}}{M_{ya,\max}} 2I_{aj} \right)^2 \right]^{\frac{1}{2}}$$

or in the shortened form, by using the factors C_{bs} for the conversion of $M_{ys}(\xi)$ and C_{ba} for the conversion of $M_{ya}(\xi)$:

$$(2.9b) \quad \frac{1}{C_{bc}} = \left[\left(\frac{M_{ys,\max}}{M_{y,\max}} \frac{1}{C_{bs}} \right)^2 + \frac{1 - \frac{N}{N_z}}{1 - 0.25 \frac{N}{N_z}} \left(\frac{M_{ya,\max}}{M_{y,\max}} \frac{1}{C_{ba}} \right)^2 \right]^{\frac{1}{2}}$$

where:

$\frac{1}{C_{bs}} = \sum_{i=1}^n \frac{M_{ys,i,\max}}{M_{ys,\max}} \frac{1}{C_{bs,i}}$, $\frac{1}{C_{bs,i}} = 2I_{si}$ and $\frac{1}{C_{ba}} = \sum_{j=1}^m \frac{M_{ya,j,\max}}{M_{ya,\max}} \frac{1}{C_{ba,j}}$, $\frac{1}{C_{ba,j}} = 2I_{aj}$ – conversion factors for the symmetric and antisymmetric moment diagram components.

When span loads are applied away from the section shear centre, the term $K_{op}(3,3)$ of the stiffness matrix K_{op} in Eq. (2.5) needs to include additional term $K_{op,F}$ related to distributed and/or concentrated loads:

$$(2.10) \quad K_{op}(3,3) = i_0^2 N_T \left(1 - \frac{N}{N_T} \right) \frac{\pi^2}{2L} + K_{op,F}$$

where:

$K_{op,F} = K_{op,q} = q_z z_q L \int_0^1 \sin^2(\pi\xi) d\xi = 0.5 q_z z_q L$ – term related to the uniformly distributed load (UDL) over the entire length of the member; $K_{op,F} = K_{op,Q} = \sum_j Q_{zj} z_{Qj} \sin^2(\pi\xi_{Qj})$ – term related to the concentrated loads (CLs) applied at the $x_{Qj} = \xi_{Qj} L$ coordinate (summation needed for multiple concentrated loads).

Substituting Eq. (2.10) to Eq. (2.5) and rearranging, as it has been done earlier, Eq. (2.8b) becomes the following one:

$$(2.11) \quad \left(\frac{M_{y,\max}}{C_{bc} M_{cr,0}} \right)^2 \frac{1}{F(N)} = 1 + \zeta_F \frac{M_{y,\max} h C_{bF}}{i_0^2 N_T \left(1 - \frac{N}{N_T} \right)}$$

or in the form of Eq. (2.8b) in which for a single type of the span load:

$$(2.12) \quad \frac{1}{C_{bc}} = \left[\frac{\left(\frac{M_{ys,\max}}{M_{y,\max}} \frac{1}{C_{bs}} \right)^2 + \frac{1 - \frac{N}{N_T}}{1 - 0.25 \frac{N}{N_T}} \left(\frac{M_{ya,\max}}{M_{y,\max}} \frac{1}{C_{ba}} \right)^2}{1 + \zeta_F \frac{M_{ys,\max} h C_{bF}}{i_0^2 N_T \left(1 - \frac{N}{N_T} \right)}} \right]^{\frac{1}{2}}$$

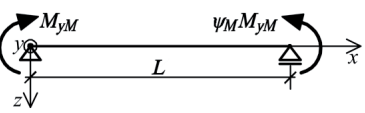
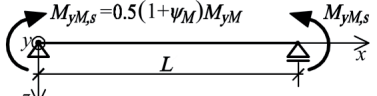
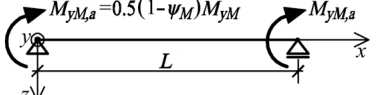
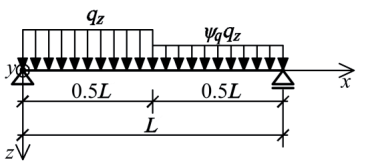
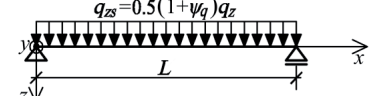
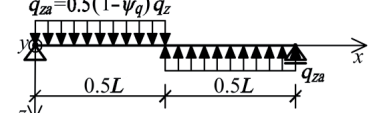
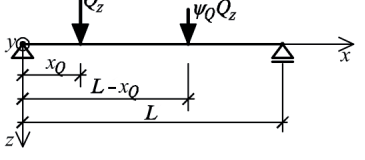
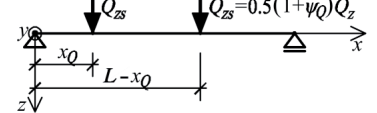
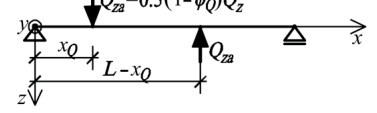
where:

$C_{bF} = \frac{2L}{\pi^2} \frac{K_{op,F}}{z_F M_{ys,\max}}$ – coefficient dependent upon the in-span load distribution, $K_{op,F}$ – term defined in Eq. (2.10) as $K_{op,q}$ or $K_{op,Q}$, $\zeta_F = z_F/h$ – dimensionless coordinate of load application away from the section shear centre, h – section depth, $M_{ys,\max}$ – maximum moment generated by the symmetric in-span load component.

2.2. PRACTICAL APPLICATIONS AND VERIFICATION

In this subchapter, some important load cases are dealt with. Eq. (2.9b) is used to present the particular solutions for unequal end moments and for span uniformly distributed loads of unequal values in two half-lengths as well as concentrated loads of unequal values in two span half-lengths, as it is shown in Table 1.

Table 1. Loading cases considered

Loading case		Component	Loading component
M		symmetric	 $M_{yM,s} = 0.5(1 + \psi_M)M_{yM}$
		antisymmetric	 $M_{yM,a} = 0.5(1 - \psi_M)M_{yM}$
q		symmetric	 $q_{zs} = 0.5(1 + \psi_q)q_z$
		antisymmetric	 $q_{za} = 0.5(1 - \psi_q)q_z$
Q		symmetric	 $Q_{zs} = 0.5(1 + \psi_Q)Q_z$
		antisymmetric	 $Q_{za} = 0.5(1 - \psi_Q)Q_z$

For load cases considered herein, the maximum moment coordinate ξ_{max} and the maximum moment itself $M_{y,max}$, the maximum moment factors $\frac{M_{ys,max}}{M_{y,max}}, \frac{M_{ya,max}}{M_{y,max}}$ as well as the dimensionless bending

moment equations $\frac{M_{ys}(\xi)}{M_{ys,max}}, \frac{M_{ya}(\xi)}{M_{ya,max}}$ for symmetric and antisymmetric components are presented in

Table A in the Appendix.

Let us first consider the very basic load case of unequal end moments, indicated by symbol M in Table 1, for which $M_{y,\max} = M_{yM}$. For this load case, Cuk and Trahair [4] presented the following relationship for the conversion factor:

$$(2.13a) \quad \frac{1}{C_{bc}} = \frac{M_{yM,s,\max}}{M_{yM,\max}} \frac{1}{C_{bs}} + \left(\frac{M_{yM,a,\max}}{M_{yM,\max}} \right)^3 \frac{1}{C_{ba}} \left(1 - 0.575 \frac{N}{N_z} \right)$$

where:

$C_{bs} = 1$, $C_{ba} = 2.50$ – conversion factors for symmetric (uniform) and antisymmetric bending moment components, $\frac{M_{yM,s,\max}}{M_{yM,\max}} = \frac{1+\psi_M}{2}$, $\frac{M_{yM,a,\max}}{M_{yM,\max}} = \frac{1-\psi_M}{2}$ – coefficients dependent upon the moment gradient ratio.

Recently, Gizejowski et al. [6] developed a refinement to Eq. (2.13a) that gives the following relationship:

$$(2.13b) \quad \frac{1}{C_{bc}} = \frac{1+\psi_M}{2} \frac{1}{C_{bs}} + \left(\frac{1-\psi_M}{2} \right)^3 \frac{1}{C_{ba}} \sqrt{\frac{1-\frac{N}{N_z}}{1-0.25\frac{N}{N_z}}}$$

in which $C_{ba} = 2.64$, instead of 2.50 like in Eq. (2.13a).

Eqs. (2.13a,b) are different from that presented herein by Eq. (2.9b). The difference is not only related to the format of the conversion factor equation but also to the form of components related to antisymmetric bending. Using Eq. (2.9b) and the direct integration of conversion factors, one can get $\frac{1}{C_{bs}} = 2I_a = 2 \int_0^1 \frac{M_{yM,s}(\xi)}{M_{yM,s,\max}} \sin^2(\pi\xi) d\xi = 1$, therefore $C_{bs} = 1$ as in Eqs. (2.12a,b), but for the moment component related to antisymmetry $\frac{1}{C_{ba}} = 2 \int_0^1 \frac{M_{yM,a}(\xi)}{M_{yM,a,\max}} \sin(\pi\xi) \sin(2\pi\xi) d\xi = \frac{32}{9\pi^2}$, therefore $C_{ba} = \frac{9\pi^2}{32} = 2.78$, instead of 2.50 or 2.64 mentioned above.

Figure 2 shows the comparison of C_{bc} as a function of the moment gradient ratio ψ_M and the critical force utilization ratio N/N_z . Solid lines indicates the present solution with $C_{ba} = 2.78$, dashed line the solution of Gizejowski et al. [6] and finally dotted line indicates that of Cuk and Trahair [4]. For $\psi_M = 1$ (uniform bending), all three solutions coincide and are identical with the closed form solution. The comparison is therefore made for nonuniform bending cases in Fig. 2 for both $\psi_M = 0$ (in-plane moment applied over one support) and $\psi_M = -1$ (in-plane moments of the same value

and direction, applied over both supports). It is clearly visible that the solutions represented by Eqs. (2.13a,b) are different from that of Eq. (9a). The differences become more pronounced when the moment gradient ratio travels from positive to negative values, with the greatest difference for $\psi_M = -1$.

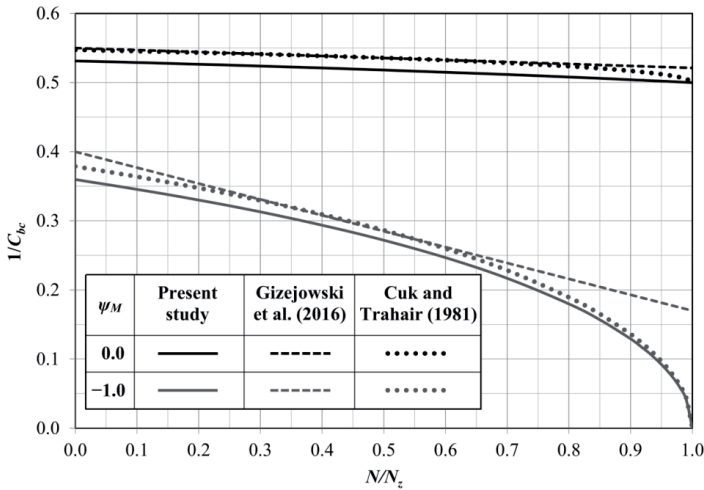


Fig. 2. Comparison of equivalent uniform moment factors for unequal end moments

The presented above solving procedure for a single load component (symbol in Table 1), giving one symmetric component and one antisymmetric component of the bending moment diagram, remains the same for more complex load cases, composed of several load components. Bijak [2] solved the flexural-torsional buckling problem of beam-columns under unequal end moments combined with UDL, using differential equilibrium equations and the modified Bobnov-Galerkin method. Such a more complex load case is a combination of load cases M and q indicated in Table 1. It consists of two symmetric moment components $M_{yM,s}(\xi) = M_{yM,s}$ and $M_{yq,s}(\xi) = M_{yq,s,max} \xi (1 - \xi)$, and one antisymmetric moment component $M_{yM,a}(\xi) = M_{yM,a}(1 - 2\xi)$. Using the developed energy method, one can get:

$$\frac{1}{C_{bs}} = 2 \int_0^1 \frac{M_{yM,s}(\xi)}{M_{ys,max}} \sin^2(\pi\xi) d\xi + 2 \int_0^1 \frac{M_{yq,s}(\xi)}{M_{ys,max}} \sin^2(\pi\xi) d\xi = \frac{M_{yM,s,max}}{M_{ys,max}} + \frac{2}{3} \left(1 + \frac{3}{\pi^2}\right) \frac{M_{yq,s,max}}{M_{ys,max}} =$$

$$\frac{M_{yM}}{M_{ys,max}} \left[\frac{1+\psi_M}{2} + \frac{2}{3} \left(1 + \frac{3}{\pi^2}\right) \mu \right]$$

$$\frac{1}{C_{ba}} = 4 \int_0^1 \frac{M_{yM,a}(\xi)}{M_{ya,max}} \sin(\pi\xi) \sin(2\pi\xi) d\xi = \frac{32}{9\pi^2} \frac{M_{yM,a,max}}{M_{yM,a,max}} = \frac{32}{9\pi^2}$$

where $M_{yq,s,max} = \mu M_{yM,s}$ and the positive sign of μ is referred to $M_{yM,s,max}$ and $M_{yq,s,max}$ being of the same sign.

Integrating the elementary conversion factors into $1/C_{bc}$ according to Eq. (2.9b), the resultant conversion factor may be drawn independently in two ranges of μ . Fig. 3 shows the graphs for these two ranges of $\mu > 0$ in Fig. 3a and $\mu < 0$ in Fig. 3b.

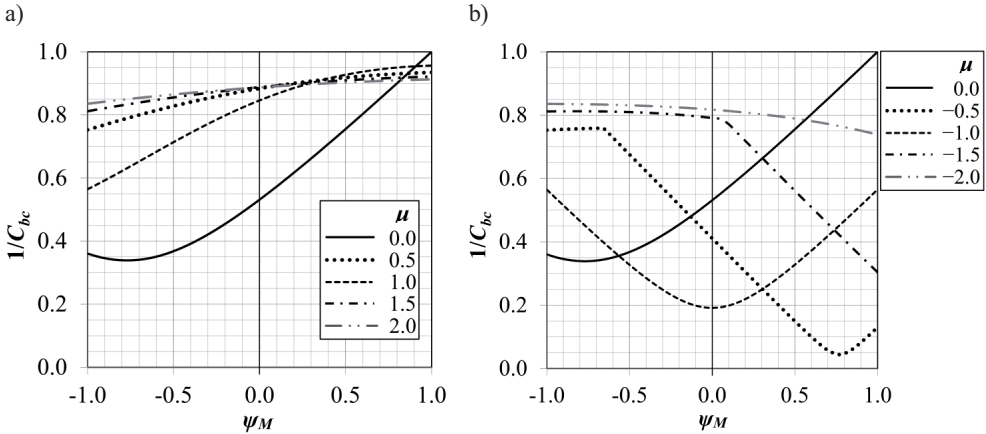


Fig. 3. Comparison of the moment conversion factor $1/C_{bc}$ for combined load cases M and q; a) symmetric components of the same signs ($\mu > 0$), b) symmetric components of the opposite signs ($\mu < 0$)

Conversion factors C_{bs} and C_{ba} are calculated for all single load cases indicated in Table 1 by symbols q and Q, using moment relationships given in Table A in the Appendix, and carrying out the integration in several ranges of ξ variable, whereas indicated. The results of present study are shown in Table 2 for all the end moments and span shear centre load cases considered. To the best authors' knowledge, the results in darkened cells have not been reported earlier in literature.

Mohri et al. [8] solved the stability problems for loads shown in Table 1 but only for the cases giving the symmetric bending moment diagram (for $\psi_M = \psi_q = \psi_Q = 1$ as indicated in the present study). The general solution presented in [8] is dependent upon two coefficients: $C_1 = \frac{\bar{C}_1}{\sqrt{k_1}}$ being the

bending moment diagram conversion factor and $C_2 = \bar{C}_2 \sqrt{\frac{G(N)}{k_1}}$ being the factor associated with the span load acting away from the section shear centre. These coefficients account for the effect of prebuckling deflections through k_1 and the effect of N on the in-plane behaviour through $G(N)$. Constants \bar{C}_1 and \bar{C}_2 are dependent upon the load case. One can notice that the former one may be

directly compared with C_{bs} of the present study (cf. Table 2). The conclusion is that for span shear centre loads, giving the symmetric moment diagrams (zero values of $1/C_{ba}$ factors), solutions presented in this study practically coincide with those predicted in earlier studies.

Table 2. Conversion factors

Symbol of load case	C_{bs} for symmetric component		C_{ba} for antisymmetric component
	Present study	Mohri et al. [8]	Present study
M	1.00	1.00	2.78
q	1.15	1.13	1.43
Q1	1.38	1.36	0.00
Q2a	1.12	1.10	1.74
Q2b	1.05	1.05	1.81

Figure 4 shows the comparison of C_{bc} for all the load cases considered in Table 1 as a function of two parameters, namely the load ratio ψ (respectively ψ_M , ψ_q and ψ_Q) and the critical force utilization ratio N/N_z . Solid lines indicates the M-case, dashed line the q-case and finally dotted and dotted-dashed lines indicate the Q-cases.

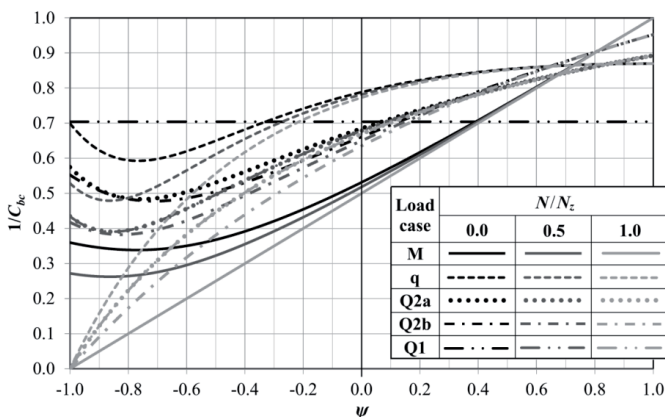


Fig. 4. Comparison of equivalent uniform moment factors for in-span shear centre loads

The off-shear load effect has been widely discussed in literature [16,17]. In this paper, the load height effect is introduced via the conversion factor, cf. Eq. (2.12). It is clear that the effect of off-

shear-centre span load plays either stabilizing or destabilizing role for buckling of beams and beam-columns, depending upon the sign of z_F and the direction of the span load. In Fig. 5, the conversion factors are compared for unequal end moments and UDL of equal values at both member half-lengths, different proportion of moments $M_{yM,max}$ and $M_{yq,max}$ being of negative and positive signs and different placement of off-shear centre UDL loads.

Exemplary IPE 360 steel section is considered for the member of 6000 mm in length. The following parameters are used: $m_{y0} = \frac{M_{yM,0,max}}{M_{cr,0}} = 1.396$; $n_{0z} = \frac{N_0}{N_z} = 0.856$; $n_{0T} = \frac{N_0}{N_T} = 0.249$; $\eta = \frac{M_{yM,0,max}h}{i_0^2 N_T} = 1.756$. Results of the calculated conversion factor are shown in Fig. 6 for $\psi_M = -1$, in Fig. 7 for $\psi_M = 0$ and in Fig. 8 for $\psi_M = 1$. Solid lines represent the top flange UDL while dashed line – bottom flange UDL and the results for the shear centre UDL are shown by dotted lines.

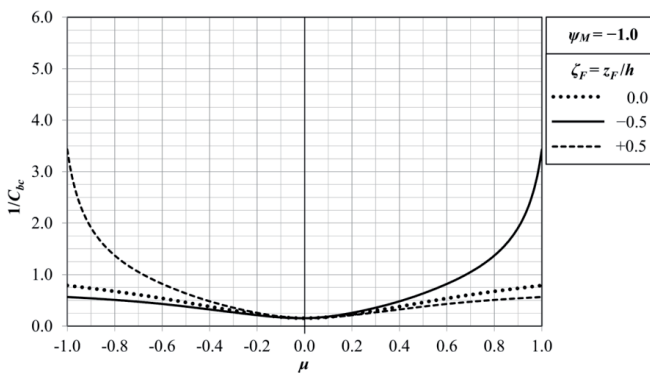


Fig. 5. Comparison of equivalent uniform moment factor for equal and of the same direction end moments, and span UDL applied away from the shear centre

For end moments producing the antisymmetric moment diagram and span UDL, one can observe that for the shear centre load the curve is symmetric with regard to the vertical axis of $\mu = 0$. When the load is applied to the top flange, the negative μ values are associated with the negative sign of q_z and the negative sign of z_q . As a result, the obtained values of $1/C_{bc}$ are lower than those obtained for the shear centre load and the bottom flange load, in the latter case being of the highest value (destabilizing effect). For positive values of μ and the top flange UDL, the sign of z_q remains the same but q_z has now the positive sign. As a result, the obtained values of $1/C_{bc}$ are higher than those obtained for the shear centre load and the bottom flange load, in the latter case being of the lowest value (stabilizing effect). Moreover, it is observed that the destabilizing effect becomes the same as the stabilizing one for positive and negative μ of the same absolute value.

For a single end moment and span UDL (Fig. 6), one can observe that for the shear centre load the curve is no longer symmetric with regard to the vertical axis of $\mu = 0$. The influence of the span UDL applied away from the shear centre is in this case similar to that of equal end moments of the same direction (cf. Fig. 5). For $\mu < 0$ and the top flange UDL, values of $1/C_{bc}$ are lower than those obtained for the shear centre load and the bottom flange load, the latter being of the highest value (destabilizing effect). For $\mu > 0$ and the top flange UDL, the obtained values of $1/C_{bc}$ are higher than those obtained for the shear centre load and the bottom flange load, in the latter case being of the lowest value (stabilizing effect). Moreover, it is observed that the destabilizing effect is no longer of that producing the stabilization for positive and negative μ of the same absolute value.

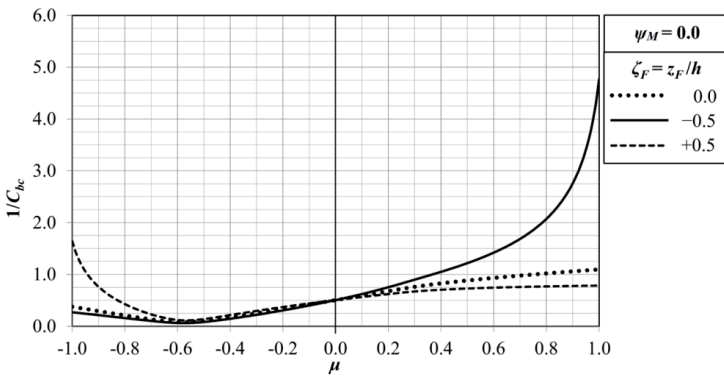


Fig. 6. Comparison of equivalent uniform moment factor for one end moment and span UDL applied away from the shear centre

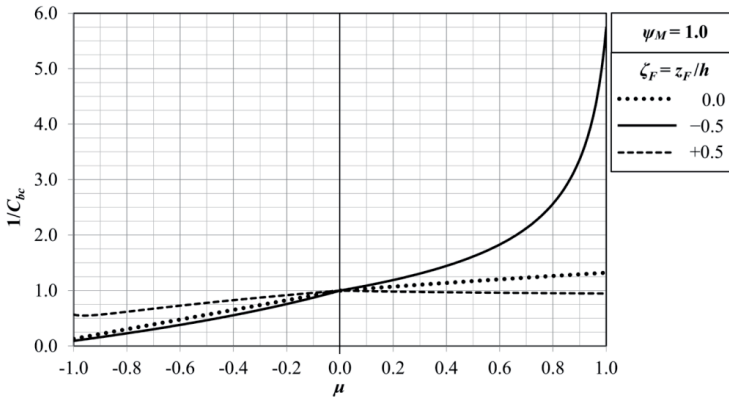


Fig. 7. Comparison of equivalent uniform moment factor for equal and of the opposite direction end moments, and span UDL applied away from the shear centre

For equal and opposite end moments and span UDL (Fig. 7), one can observe that for the shear centre load the curve and the influence of the span UDL applied away from the shear centre in this case is similar to that of a single end moment (cf. Fig. 6).

3. SUMMARY AND CONCLUSIONS

A linear stability model for the flexural-torsional buckling of beam-columns was presented. The formulation is based on the classical energy equation, presented in the form of LEA and solved analytically for different load cases presented in Table 1. The novelty of present study yields from the fact that any complex load case composed of end moments and span loads is represented by a combination of symmetric and antisymmetric components, therefore the field moment $M_{yM}(\xi)$ due to applied end moments is a sum of symmetric and antisymmetric components, $M_{yM,s}(\xi)$ and $M_{yM,a}(\xi)$ respectively, and the field moment due to applied span loads F_{zk} (F_{zk} symbol refers to components q_{zi} and Q_{zj}) is also a sum of symmetric and antisymmetric components, $M_{yF,s}(\xi)$ and $M_{yF,a}(\xi)$ respectively. The field moments are presented as functions of load factors ψ_M, ψ_q, ψ_Q describing the moment diagrams asymmetry under single loads of end moments, span UDL and span CL, the last two unequal in both half-lengths. Moment dependent conversion factors C_{bs} (referred to the symmetric moment components) and C_{ba} (referred to the antisymmetric moment components) have been evaluated for single load cases. Factors C_{bs} were compared to those existing in the literature and a good agreement have been shown. To the best authors' knowledge, factors C_{ba} have not yet been presented in the literature for span loads.

More complex load cases were also dealt with on the example of unequal end moments and span UDL over the entire member length. Two different span load signs were considered, namely positive when its direction coincides with the positive direction of the z -axis (the bending moment is of the opposite sign to that produced by end moments) and negative when the load is directed oppositely. The effect of load height was also investigated showing that the off-shear load has either destabilizing effect or stabilizing effect on the critical moment. This was conveniently looked at through the observations of the influence of load sign and load height coordinate sign on the resultant moment conversion factor $1/C_{bc}$.

The developed elastic buckling interaction curves N - M_y play an important role in the buckling resistance assessment of imperfect members using the so-called General method (GM) introduced in the clause 6.3.4 of current Eurocode 3 [5]. This method has been effectively used only for simple member loads since the general solution for elastic buckling interaction equation of beam-columns

under compression and major axis bending was not widely investigated in the literature. The present study is a starting point for further investigations into the improvement of herein developed solution, replacing the linear eigenproblem formulation (LEA) by its nonlinear eigenproblem counterpart (NEA).

REFERENCES

1. R. Bijak, "The lateral buckling of simply supported unrestrained bisymmetric I-shape beams", *Archives of Civil Engineering* 61(4): 127-140, 2015.
2. R. Bijak, "Lateral-torsional buckling of simply supported bisymmetric beam-columns", *Journal of Civil Engineering, Environment and Architecture* 34(3I): 461-470, 2017.
3. M.A. Bradford, P.E. Cuk, M.A. Gizejowski, N.S. Trahair, "Inelastic lateral-buckling of beam-columns", *Journal of Structural Engineering* 113(11): 2259-2277, 1987.
4. P.E. Cuk, N.S. Trahair, "Elastic buckling of beam-columns with unequal end moments", *Civil Engineering Transactions, Institution of Engineers, Australia*, 3: 166-171, 1981.
5. Eurocode 3. EN 1993-1-1: 2005 Design of steel structures, Part 1-1: General rules and rules for buildings, CEN, Brussels, 2005.
6. M. Gizejowski, Z. Stachura, J. Uziak, "Elastic flexural-torsional buckling of beams and beam-columns as a basis for stability design of members with discrete rigid restraints", in A. Zingoni (ed.), *Insights and Innovations in Structural Engineering, Mechanics and Computation*, London, Taylor & Francis Group: 261-262 (e-book on CD: 738-744), 2016.
7. M. Gizejowski, J. Uziak, "On elastic buckling of bisymmetric H-section steel elements under bending and compression", Invited paper in A. Zingoni (ed.), *Advances in Engineering Materials, Structures and Systems: Innovations, Mechanics and Applications*, London, Taylor & Francis Group: 1160-1167, 2019.
8. F. Mohri, Ch. Bouzerira, M. Potier-Ferry, "Lateral buckling of thin-walled beam-column elements under combined axial and bending loads", *Thin-Walled Structures* 46(3): 290-302, 2008.
9. F. Mohri, N. Damil, M. Potier-Ferry, "Buckling and lateral buckling interaction in thin-walled beam-column elements with mono-symmetric cross sections", *Applied Mathematical Modelling* 37: 3526-3540, 2013.
10. Y.L. Pi, N.S. Trahair, S. Rajasekaran, "Energy equation for beam lateral buckling", *Journal of Structural Engineering* 118 (6): 1462-1479, 1992.
11. Y.L. Pi, M.A. Bradford, "Effects of approximations in analyses of beams of open thin-walled cross-section", *International Journal for Numerical Methods in Engineering*, "Part I: Flexural-torsional stability" 51:757-772, "Part II: 3-D nonlinear behavior" 51:773-790, 2001.
12. Y.L. Pi, N.S. Trahair, "Prebuckling deflections and lateral buckling", *Journal of Structural Engineering*, "Part I: Theory" 118(11): 2949-2966, "Part II: Applications" 118(11):2967-2985, 1992.
13. Y.L. Pi, N.S. Trahair, "Nonlinear inelastic analysis of steel beam-columns", *Journal of Structural Engineering*, "Part I: Theory" 120(7):2041-2061, "Part II: Applications" 120(7): 2062-2085, 1994.
14. M.A.M. Torkamani, E.R. Roberts, "Energy equations for elastic flexural-torsional buckling analysis of plane structures", *Thin-Walled Structures* 47: 463-473, 2009.
15. P. Van Binh, D.H. Minh, G.S. Sergeevich, N.V. Duc, "Boundary of stability region of a thin-walled beam under complex loading condition", *International Journal of Mechanical Sciences* 122: 355-361, 2017.
16. N. S. Trahair, "Flexural-torsional buckling of structures". Boca Raton: CRC Press, 1993.
17. N.S. Trahair, M.A. Bradford, D. A. Nethercot, L. Gardner, "The behaviour and design of steel structures to EC3". Second ed. London-New York: Taylor and Francis, 2008.

Appendix

Table A. Description of bending moment equations for load cases from Table 1

Symbol k indicating load case ^{a)}	ξ_{\max}	$M_{y,\max}$	$\frac{M_{ys,\max}}{M_{y,\max}}$	$\frac{M_{ys}(\xi)}{M_{y,\max}}$	Range
			$\frac{M_{ya,\max}}{M_{y,\max}}$	$\frac{M_{ya}(\xi)}{M_{y,\max}}$	
M	0	M_y	$\frac{1 + \psi_M}{2}$	1	$\xi \leq 1$
			$\frac{1 - \psi_M}{2}$	$1 - 2\xi$	$\xi \leq 1$
q	$\frac{3 + \psi_q}{8}$	$\frac{q_z L^2 (3 + \psi_q)^2}{8 \cdot 16}$	$8 \frac{1 + \psi_q}{(3 + \psi_q)^2}$	$4\xi(1 - \xi)$	$\xi \leq 1$
			$2 \frac{1 - \psi_q}{(3 + \psi_q)^2}$	$8\xi(1 - 2\xi)$	$\xi \leq 1/2$
Q1	$\frac{1}{2}$	$\frac{Q_z L}{4}$	1	2ξ	$\xi \leq 1/2$
				$2(1 - \xi)$	$\xi > 1/2$
Q2a	$\frac{1}{3}$	$\frac{Q_z L}{9} (2 + \psi_Q)$	$\frac{3}{2} \frac{1 + \psi_Q}{2 + \psi_Q}$	3ξ	$\xi \leq 1/3$
				1	$1/3 < \xi < 2/3$
Q2b	$\frac{1}{4}$	$\frac{Q_z L}{16} (3 + \psi_Q)$	$2 \frac{1 + \psi_Q}{3 + \psi_Q}$	$3(1 - \xi)$	$\xi \geq 2/3$
			$\frac{1}{2} \frac{1 - \psi_Q}{2 + \psi_Q}$	3ξ	$\xi \leq 1/3$
Q2b	$\frac{1}{4}$	$\frac{Q_z L}{16} (3 + \psi_Q)$		$3(1 - 2\xi)$	$1/3 < \xi < 2/3$
				$-3(1 - \xi)$	$\xi \geq 2/3$
Q2b	$\frac{1}{4}$	$\frac{Q_z L}{16} (3 + \psi_Q)$	$2 \frac{1 + \psi_Q}{3 + \psi_Q}$	4ξ	$\xi \leq 1/4$
				1	$1/4 < \xi < 3/4$
Q2b	$\frac{1}{4}$	$\frac{Q_z L}{16} (3 + \psi_Q)$		$4(1 - \xi)$	$\xi \geq 3/4$
			$\frac{1 - \psi_Q}{3 + \psi_Q}$	4ξ	$\xi \leq 1/4$
				$2(1 - 2\xi)$	$1/4 < \xi < 3/4$
				$-4(1 - \xi)$	$\xi \geq 3/4$

^{a)} Q1 – load Q_z applied at $x_Q = L/2$ (symmetric load case with no antisymmetric component)
 Q2a – load Q_z applied at $x_Q = L/3$ and $\psi_Q Q_z$ applied at $L - x_Q = 2L/3$
 Q2b – load Q_z applied at $L/4$ and load $\psi_Q Q_z$ applied at $L - x_Q = 3L/4$

Table B. Description of bending moment equations for the combination of unequal end moments and uniformly distributed load over the whole member length

ξ_{\max}	$\frac{4\mu + \psi_M - 1}{8\mu}$	0			$\frac{4\mu + \psi_M - 1}{8\mu}$
Range μ	$\mu < \frac{\psi_M - 1}{4}$	$\mu \geq \frac{\psi_M - 1}{4}$	0	$\mu \leq \frac{1 - \psi_M}{4}$	$\mu > \frac{1 - \psi_M}{4}$
$M_{ys,\max}$	$\max\left(\frac{1 + \psi_M}{2}; \frac{1 + \psi_M}{2} + \mu\right) M_{yM}$		$\frac{1 + \psi_M}{2}$	$\left(\frac{1 + \psi_M}{2} + \mu\right) M_{yM}$	
$M_{y,\max}$	$\max\left[1; 1 + \frac{(4\mu + \psi_M - 1)^2}{16\mu}\right] M_{yM}$	M_{yM}			$\left[1 + \frac{(4\mu + \psi_M - 1)^2}{16\mu}\right] M_{yM}$
$\frac{M_{yq,s,\max}}{M_{ys,\max}}$	$\frac{2\mu}{\max(1 + \psi_M; 1 + \psi_M + 2\mu)}$		0	$\frac{2\mu}{1 + \psi_M + 2\mu}$	
$\frac{M_{yM,s,\max}}{M_{ys,\max}}$	$\frac{1 + \psi_M}{\max(1 + \psi_M; 1 + \psi_M + 2\mu)}$		1	$\frac{1 + \psi_M}{1 + \psi_M + 2\mu}$	
$\frac{M_{ys,\max}}{M_{y,\max}}$	$\frac{\max\left(\frac{1 + \psi_M}{2}; \frac{1 + \psi_M}{2} + \mu\right)}{\max\left[1; 1 + \frac{(4\mu + \psi_M - 1)^2}{16\mu}\right]}$	$\max\left(\frac{1 + \psi_M}{2}; \frac{1 + \psi_M}{2} + \mu\right)$	$\frac{1 + \psi_M}{2}$	$\frac{1 + \psi_M}{2} + \mu$	$\frac{8\mu(1 + \psi_M + 2\mu)}{16\mu + (4\mu + \psi_M - 1)^2}$
$\frac{M_{ya,\max}}{M_{y,\max}}$	$\frac{(1 - \psi_M)/2}{\max\left[1; 1 + \frac{(4\mu + \psi_M - 1)^2}{16\mu}\right]}$	$\frac{1 - \psi_M}{2}$			$\frac{8\mu(1 - \psi_M)}{16\mu + (4\mu + \psi_M - 1)^2}$
$\frac{M_{ys}(\xi)}{M_{ys,\max}}$	$\frac{1 + \psi_M + 8\mu\xi(1 - \xi)}{\max(1 + \psi_M; 1 + \psi_M + 2\mu)}$		1	$\frac{1 + \psi_M + 8\mu\xi(1 - \xi)}{1 + \psi_M + 2\mu}$	
$\frac{M_{ya}(\xi)}{M_{ya,\max}}$	$1 - 2\xi$				

LIST OF FIGURES AND TABLES:

Fig. 1. Coordinate system used in beam theory

Rys. 1. Układ współrzędnych przyjęty w teorii belek

Fig. 2. Comparison of equivalent uniform moment factors for unequal end moments

Rys. 2. Porównanie współczynników równoważnego stałego momentu w przypadku momentów końcowych o różnych wartościach

Fig. 3. Comparison of the moment conversion factor $1/C_{bc}$ for combined load cases M and q; a) symmetric components of the same signs ($\mu > 0$), b) symmetric components of the opposite signs ($\mu < 0$)

Rys. 3. Porównanie współczynnika konwersji momentu $1/C_{bc}$ dla połączonych przypadków obciążenia M i q; a) składowe symetryczne tych samych znaków ($\mu > 0$), b) składowe symetryczne przeciwnych znaków ($\mu < 0$)

Fig. 4. Comparison of equivalent uniform moment factors for in-span shear centre loads

Rys. 4. Porównanie współczynników równoważnego stałego momentu w odniesieniu do obciążeń przyłożonych w środku ścinania

Fig. 5. Comparison of equivalent uniform moment factor for equal and of the same direction end moments, and span UDL applied away from the shear centre

Rys. 5. Porównanie współczynnika równoważnego stałego momentu dla równych i o tych samych zwrotach momentów końcowych oraz obciążenia przęsłowego UDL przyłożonego poza środkiem ścinania

Fig. 6. Comparison of equivalent uniform moment factor for one end moment and span UDL applied away from the shear centre

Rys. 6. Porównanie współczynnika równoważnego stałego momentu w przypadku pojedynczego momentu końcowego oraz obciążenia przęsłowego UDL przyłożonego poza środkiem ścinania

Fig. 7. Comparison of equivalent uniform moment factor for equal and of the opposite direction end moments, and span UDL applied away from the shear centre

Rys. 7. Porównanie współczynnika równoważnego stałego momentu dla równych i o przeciwnych zwrotach momentów końcowych oraz obciążenia przęsłowego UDL przyłożonego poza środkiem ścinania

Tab. 1. Loading cases considered

Tab. 1. Rozważone przypadki obciążenia

Tab. 2. Conversion factors

Tab. 2. Współczynniki konwersji

Tab. A. Description of bending moment equations for load cases from Table 1

Tab. A. Opis równań momentów zginających dla przypadków obciążeń z Tabeli 1

Tab. B. Description of bending moment equations for the combination of unequal end moments and uniformly distributed load over the whole member length

Tab. B. Opis równań momentów zginających dla kombinacji momentów końcowych o różnych wartościach i obciążenia równomiernie rozłożonego na całej długości pręta

GIĘTNO-SKRĘTNE WYBOCZENIE SPRĘŻYSTE DWUTEOWYCH ELEMENTÓW STALOWYCH NIESTĘŻONYCH POMIĘDZY SKRAJNYMI PODPORAMI

Słowa kluczowe: element stalowy, przekrój dwuteowy bisymetryczny, zachowanie sprężyste, zwichrzenie, klasyczne równanie energii, wyoboczenie giętno-skrętne

STRESZCZENIE:

Na podstawie teorii prętów cienkościennych Własowa w artykule przedstawiono zagadnienia stateczności sprężystej stalowych elementów o przekrojach dwuteowych bisymetrycznych, poddanych ścisnaniu i zginaniu względem osi większej bezwładności przekroju. Ponieważ rozwiązanie ściśle zagadnienia zwichrzenia oraz wyoboczenia giętno-skrętnego elementów ściskanych i zginanych można wyznaczyć tylko w odniesieniu do prostych przypadków obciążeń, w przypadkach bardziej złożonych obciążeń wykorzystuje się metody przybliżone – zarówno analityczne jak i numeryczne. Badania przedstawione w pracy dotyczą analitycznej metody energetycznej odniesionej do dowolnego złożonego przypadku obciążenia, który traktuje się jako superpozycję symetrycznej i antysymetrycznej części obciążenia.

W pierwszej kolejności przedstawiono różne sformułowania, tak zwane alternatywne i klasyczne, równań dotyczących energii odkształcenia i obciążenia w wypadku zwichrzenia sprężystego belek zginanych. Dokładniejsze klasyczne równanie energii sformułowane dla belek zginanych o przekroju dwuteowym bisymetrycznym rozszerzono o wpływ siły podłużnej ściskającej w celu rozwiązania problemu giętno-skrętnego wyoboczenia elementów ściskanych i zginanych oraz przedstawiono w postaci funkcji pochodnych kąta skręcenia ϕ i przemieszczenia liniowego v . Następnie, po przyjęciu funkcji kształtu kąta skręcenia ϕ oraz przemieszczenia v tak, aby obejmowały postacie zwichrzenia belki odpowiadające symetrycznemu i antysymetrycznemu rozkładowi momentu zginającego, wyprowadzono macierzowe kryterium utraty stateczności pręta w ujęciu liniowego problemu wartości własnych (LEA). Ostatecznie przedstawiono jawną postać rozwiązania liniowego problemu wartości własnych zależną od symetrycznej i antysymetrycznej części momentu zginającego. Otrzymane rozwiązanie porównano z wynikami uzyskanymi z innych badań i stwierdzono dobrą zgodność.

Opracowane krzywe stateczności sprężystej elementów ściskanych i zginanych odgrywają ważną rolę w ocenie nośności wyoboczeniowej nieidealnych elementów ściskanych i zginanych przy użyciu tak zwanej metody ogólnej (z ang. General Method), wprowadzonej w eurokodzie stalowym EN 1993-1-1:2005. Metodę tę stosuje się skutecznie tylko w przypadku prostych obciążeń prętów, ponieważ ogólne rozwiązanie równania stateczności sprężystej elementów ściskanych i zginanych nie było szeroko badane w literaturze. Artykuł jest punktem wyjścia do dalszych badań nad ulepszeniem opracowanego rozwiązania, polegającym na zastąpieniu liniowej formuły problemu wartości własnych (LEA) jej odpowiednikiem wynikającym z nieliniowego problemu wartości własnych (NEA).

Received: 20.10.2020, Revised: 03.11.2020